Localized nonlinear optical modes and the corresponding support structures: Exact solutions to the nonlinear Schrödinger equation with external potentials

B. A. Malomed[1] Y. A. Stepanyants[2]

Abstract – **Two analytical techniques for the generation of wide classes of exact solutions of the nonlinear Schrödinger equation (NLSE) containing an external potential are proposed. Both methods are illustrated by a variety of localized solutions, including solitary optical vortices, for both the self-focusing and self-defocusing nonlinearities. The stability of solutions was tested by direct numerical simulations of the NLSE; the existence of stable localized modes was confirmed through the simulation.**

1 INTRODUCTION

It is well known that the propagation of electromagnetic waves in nonlinear optical waveguides is described by the nonlinear Schrödinger equation (NLSE) [1]. In the spatial domain, one- and two-dimensional (1D and 2D) NLSEs apply, respectively, to the planar and bulk waveguides. Along with the cubic nonlinear term, they may include a linear potential that represents a transverse structure induced by the local modulation of the refractive index in the waveguide [2]. The dimensionless form of the 2D NLSE is

$$i\frac{\partial\psi}{\partial t}=-\frac{\partial^2\psi}{\partial x^2}+s\frac{\partial^2\psi}{\partial y^2}+\sigma|\psi|^2\psi+U(x,y)\psi, \qquad (1)$$

where $U(x, y)$ is the external potential, $s = +1$ and -1 correspond to the hyperbolic and elliptic types of the NLSE, both cases being physically meaningful [1], and $\sigma = +1$ (-1) refer to the self-defocusing (focusing) sign of the Kerr nonlinearity. In most applications to optics, the evolution variable t is actually the propagation distance z.

Exact solutions to the NLSE can be rarely found in the presence of external potentials, although the knowledge of such exact solutions is valuable for various purposes. Here we propose two analytical techniques for the generation of wide classes of exact solutions in this context. The first approach is the development of the Kondrat'ev–Miller method [3], applied to the 1D version of Equation (1), with U and φ depending only on x. This method is based on the similarity between the stationary version of the NLSE and the integrable Gardner equation [4]:

$$\frac{\partial\phi}{\partial\tau}+\frac{\partial}{\partial\xi}\left(\frac{\partial^2\phi}{\partial\xi^2}+c\phi-\phi^2-\sigma\phi^3\right)=0. \qquad (2)$$

All solutions of the latter equation, both stationary and nonstationary ones, can be used to generate exact solutions to the 1D NLSE, along with the potentials supporting such solutions.

The second method is based on the solution of the "inverse problem" for the NLSE, i.e. construction of a potential which gives rise to the desirable solution representing the field distribution. Systematic results are presented for 1D and 2D cases. Both methods are illustrated by a variety of localized solutions, including solitary optical vortices, for both the self-focusing and self-defocusing nonlinearities. The stability of the so generated solutions was verified by direct simulations of Equation (1).

2 STATIONARY SOLUTIONS TO THE 1D NLSE FROM SOLUTIONS OF THE AUXILIARY GARDNER EQUATION

Looking for 1D solutions to Equation (1) in the form of $\varphi(x,t) = \varphi(x)\exp(-i\mu t)$ reduces Equation (1) to the following equation for the real function $\varphi(x)$:

$$\frac{d^2\varphi}{dx^2}+\mu\varphi=\sigma\varphi^3+U(x)\varphi. \qquad (3)$$

Following the Kondrat'ev–Miller method [3], in parallel to Equation (3) we consider the Gardner equation (2), re-written as follows:

$$\frac{\partial^2\phi}{\partial\xi^2}+c\phi=\sigma\phi^3+\left[\Phi(\xi,\tau)-\frac{1}{\Phi(\xi,\tau)}\int_0^{\xi}\frac{\partial\Phi}{\partial\tau}d\xi'\right]\phi. \qquad (4)$$

[1] Department of Physical Electronics, School of Electrical Engineering, Faculty of Engineering, Tel Aviv University, Tel Aviv, 69978, Israel, e-mail: Malomed@eng.tau.ac.il, tel.: +972 3 640 6413, fax: +972 3 641 0189.
[2] Department of Mathematics and Computing, Faculty of Sciences, University of Southern Queensland, Toowoomba, QLD, 4350, Australia, e-mail: Yury.Stepanyants@usq.edu.au, tel.: +61 7 4631 5548, fax: +61 7 4631 5550.

978-1-4244-7368-7/10/$26.00 ©2010 IEEE

where $\Phi(\xi, \tau)$ is one of its exact solutions. Note that formal temporal variable τ in the auxiliary Gardner equation (2) or (4) has nothing to do with physical time t in the NLSE (1).

There is the one-to-one correspondence between equations (3) and (4): $\varphi \leftrightarrow \phi$, $x \leftrightarrow \xi$, $\mu \leftrightarrow c$. The term in the square brackets of Equation (4) can be formally identified with external potential $U(\xi, \tau)$, which depends, in the general case, on free parameter τ. In particular cases, when a stationary solution of the Gardner equation is substituted into Equation (4) as a trial solution $\Phi(\xi)$, the potential $U(\xi)$ is simply equal to $\Phi(\xi)$ and is independent of τ.

2.1 Soliton solution of the Gardner equation

As the simplest illustrative example, we consider a stationary solution to the Gardner equation in the form of a soliton. In the case of the attractive nonlinearity, $\sigma = -1$, this solution is (see Ref. [5] where other cases are also presented in detail):

$$\Phi_{\pm}(\xi) = \frac{-3\nu^2}{1 \pm \sqrt{1 + 9\nu^2/2}\cosh(\nu\xi)}, \qquad (5)$$

where ν is a free parameter, and $c = -\nu^2$ in this case. This solution in terms of Φ^2, along with the corresponding potential, $U(\xi)$, in Equation (3) are shown in Figure 1.

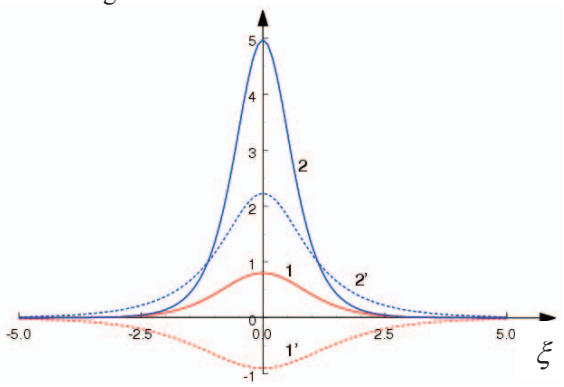

Figure 1: Solution (5) with $\nu = 1$ in terms of $\Phi^2(\xi)$ (solid lines) and the corresponding potential, $U(\xi)$ (broken lines). Lines 1, 1' and 2, 2' pertain, respectively, to signs plus and minus in Equation (5).

The stability of soliton solutions (5) was tested via direct simulations of Equation (1). The expected instability of solution $\Phi_{-}(\xi)$ sitting at the maximum of the potential (see lines 2 and 2' in Figure 1) was corroborated. Meanwhile, it was revealed, in agreement with the expectation, that soliton solution $\Phi_{+}(\xi)$ sitting at the minimum of the potential (see lines 1 and 1' in Figure 1) is *stable* against strong perturbations (up to 10% with respect to the soliton amplitude). The amplitude of the stable perturbed soliton, $\Phi_{+}(\xi)$, varied in time around an average value and remained within the same range of the deviation from the stationary value as the initial perturbation. Details of simulations and many other examples can be found in [5].

2.2 Breather solution of the Gardner equation

As the next example, we consider nonstationary solution to the Gardner equation in the form of a breather. Such solution exists only in the case of the attractive nonlinearity, $\sigma = -1$ [6]:

$$\Phi(\xi,\tau) = -\frac{4}{3}ab\frac{A(\xi,\tau) + B(\xi,\tau)}{C(\xi,\tau) - D(\xi,\tau)}, \qquad (6)$$

where

$$A(\xi,\tau) = \frac{b\cosh\eta\cos\chi + a\cos\theta\cosh\varphi}{a\sin\theta\cosh\varphi + b\sinh\eta\cos\chi},$$

$$B(\xi,\tau) = \frac{b\sinh\eta\sin\chi + a\sin\theta\sinh\varphi}{a\cos\theta\sinh\varphi - b\cosh\eta\sin\chi},$$

$$C(\xi,\tau) = \frac{b\cosh\eta\sin\chi - a\cos\theta\sinh\varphi}{a\sin\theta\cosh\varphi + b\sinh\eta\cos\chi},$$

$$D(\xi,\tau) = \frac{b\sinh\eta\cos\chi + a\sin\theta\cosh\varphi}{a\cos\theta\sinh\varphi - b\cosh\eta\sin\chi},$$

$\eta = (a\sqrt{2}/3)(x - x_0 - V\tau)$, $\theta = (b\sqrt{2}/3)(x - x_{ph} - \upsilon\tau)$, $V = (2/9)(a^2 - 3b^2)$, $\upsilon = (2/9)(3a^2 - b^2)$, $c = 0$, $\varphi + i\chi = (1/2)\ln[(i + 2\lambda)/(i - 2\lambda)]$, and $\lambda = (a + ib)/2$.

The quantities x_0 and x_{ph} specify the initial position and phase of the breather. The breather is a two-parametric solution determined by arbitrary real parameters a and b. In the "moving reference frame", when $\eta = \text{const}$, the breather is periodic in τ with period $T_{br} = 27\pi/[2\sqrt{2}b(a^2 + b^2)]$. In general, it looks like a wavetrain propagating with group velocity V, whereas υ plays the role of the phase velocity. However, within the framework of the NLSE, the breather is a *stationary* field whose shape is determined by parameter τ.

For $a >> b$, the breather's behaviour in the plane ξ, τ resembles the interaction of two solitons of different polarities, as shown in Figure 2a. The breather's shape becomes very asymmetric when a is comparable to b. In the opposite case of $b >> a$, the breather represents a rather symmetric envelope soliton on top of a high-frequency career wave [6].

The presence of free parameter τ in the solution gives an opportunity for fine tuning of the desirable wave field and corresponding potential. In particular, one can smoothly vary the potential from the well to the hump, which results in stable and unstable field distributions, respectively. An example of the stable field distribution is depicted in Figure 2b.

In a similar manner, stationary or nonstationary periodic solutions of the Gardner equation can be used to construct stationary solutions to the NLSE, along with the corresponding potentials.

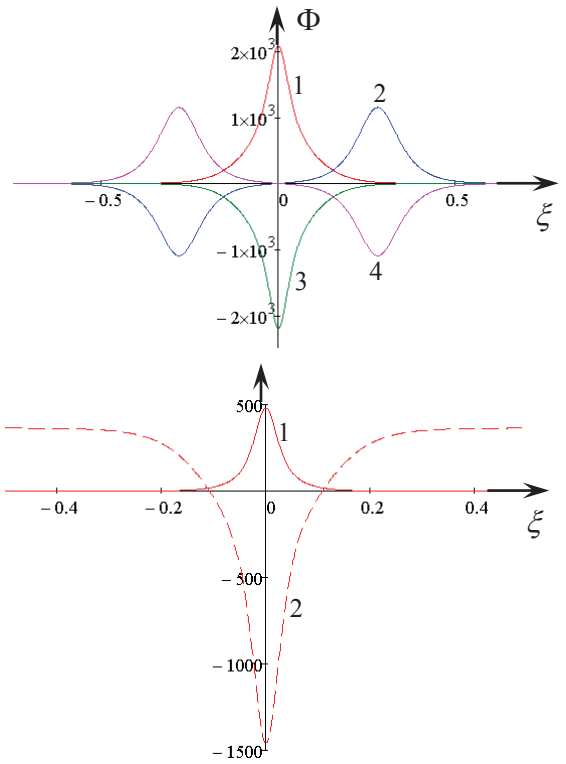

Figure 2: a) Breather solution (6) in the "moving reference frame", where $\eta = \text{const}$, for $a = 40$, $b = 0.4$ and different values of τ, *viz.*, $\tau = 0$ (line 1), $T_{br}/4$ (line 2), $T_{br}/2$ (line 3), and $3T_{br}/4$ (line 4) (the breathers depicted by lines 2 and 4 are ten times magnified). b) Solution (6), shown as $\Phi^2(\xi,0)\cdot 10^{-4}$ (solid line 1), and the corresponding potential $U(\xi)$ (broken line 2).

3 CONSTRUCTION OF THE SUPPORTING POTENTIAL IN THE NLSE FOR A GIVEN DISTRIBUTION OF THE WAVE FIELD

An arbitrary distribution of the stationary wave field, $\varphi(x,y)$, can be made an exact solution to the stationary NLSE (1) with $\partial/\partial t = 0$, if the potential in the equation is chosen accordingly:

$$U(x,y) = \frac{1}{2|\varphi|^2}\left(\frac{\partial^2|\varphi|^2}{\partial x^2} - s\frac{\partial^2|\varphi|^2}{\partial y^2}\right) - \frac{|\varphi_x|^2 - s|\varphi_y|^2}{|\varphi|^2} - \sigma|\varphi|^2. \quad (7)$$

Among such solutions only those are of practical interest which are stable and give rise to non-singular potentials. Several examples are presented below to demonstrate that this, seemingly trivial, approach may produce essential results of practical interest.

3.1 The one-dimensional Gaussian wave field

As the simplest example, we take a Gaussian distribution of the stationary wave field, which may be a case of obvious interest to applications, $\varphi(x) = A\exp(-x^2/l^2)$. Substituting this trial function into 1D version of Equation (7) with $\partial/\partial y = 0$, one finds:

$$u(\zeta) \equiv \frac{U(\zeta)}{A^2} = \frac{4}{A^2 l^2}\left(\zeta^2 - \frac{d}{2}\right) - \sigma\exp\left(-2\zeta^2\right), \quad (8)$$

where $\zeta = x/l$, and d is the spatial dimension.

The dimensionless potential, $u(\zeta)$, depends on the parameter $S \equiv Al$ for each sign of σ. In the case of the repulsive nonlinearity ($\sigma = 1$), the potential has only one well for all values of S (see line 1' in Figure 3), with the shape of the well asymptotically, at $\zeta \to \infty$, approaching the parabolic profile. This provides for the stability of the Gaussian solution against small perturbations, as confirmed by direct numerical calculations of the nonstationary 1D NLSE.

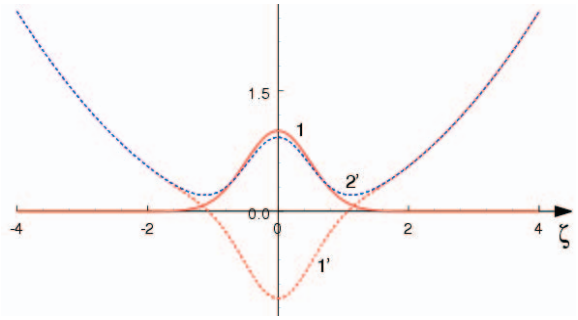

Figure 3: The Gaussian solution (line 1), shown as, $\varphi^2(\zeta)/A^2$, and the respective potentials $u(\zeta)$ (lines 1' and 2'), for $\sigma = 1$ and $\sigma = -1$, respectively, and $S = 5$.

However, in the case of the attractive nonlinearity ($\sigma = -1$), the potential features a *double-well* shape, when S exceeds a threshold value, $S_{thr} = \sqrt{2}$, (see line 2' in Figure 3), which indicates a possible instability of the Gaussian solution. Direct simulation of the nonstationary 1D NLSE reveals, in accordance with the expectation, that the Gaussian solution is stable for $S \le S_{thr}$. For larger values of S, the solution becomes unstable indeed. It preserves its shape at $t \le 20$, and then spontaneously splits into two pulses which quasi-regularly oscillate relative to each other.

In a similar manner, several other stationary solutions were used to generate the corresponding potential functions for the 1D NLSE [5]. Among them are a derivative-Gaussian function, and a combination of a periodic comb and the Gaussian. Their stability was also tested against small perturbations, both stable and unstable solutions being found.

3.2 The two-dimensional Gaussian wave field

The simplest example in the 2D case is based on the axisymmetric Gaussian distribution of the stationary wave field, $\varphi(r) = A\exp(-r^2/l^2)$, where $r^2 = x^2 + y^2$. Substituting this ansatz into Equation (7) with $s = -1$, one arrives at the same Equation (8) with $d = 2$, where now $\zeta = r/l$. A similar solution was obtained in Ref. [7] in a different way, and its stability was verified by direct numerical simulation.

3.3 Optical vortices

Other examples of 2D optical patterns are *vortices*. The simplest among them is the unitary vortex, with topological charge $J = 1$ (it may be treated as a 2D counterpart of the antisymmetric 1D derivative-Gaussian solitary wave mentioned above): $\varphi(x, y) = A(x + iy)^2\exp(-r^2/l^2)$. Substituting this ansatz into Equation (7) with $s = -1$, one finds:

$$u(\zeta) \equiv \frac{U(\zeta)}{A^2 l^2} = \frac{4}{A^2 l^4}\left(\zeta^2 - 2\right) - \sigma\zeta^2 \exp\left(-2\zeta^2\right). \quad (9)$$

A *double-vortex* solution, with $J = 2$, along with the corresponding potential, can be readily constructed in the same way. In this case, the trial function is $\varphi(x, y) = A(x + iy)\exp(-r^2/l^2)$, and the corresponding supporting potential being

$$u(\zeta) \equiv \frac{U(\zeta)}{A^2 l^4} = \frac{4}{A^2 l^6}\left(\zeta^2 - 3\right) - \sigma\zeta^4 \exp\left(-2\zeta^2\right). \quad (10)$$

3.4 The 2D hyperbolic NLSE

The propagation of a spatio-temporal light signal in a planar waveguide with the Kerr nonlinearity and normal group-velocity dispersion obeys the 2D NLSE (1) with the linear operator of the hyperbolic type [1]. As has been demonstrated in Ref. [8], the addition of a specially devised linear-potential term to this equation makes it possible to find exact delocalized solutions for X-waves formally described by Equation (1) with $s = 1$, where, in this case, $t \equiv z$ plays the role of the propagation distance, x is the transverse coordinate in the waveguide's plane, y is the reduced-time variable, $-\sigma$ is the sign of the Kerr coefficient, and $U(x, y)$ is the potential induced by a local modulation of the refractive index (in particular, the modulation in the temporal direction may be provided, via the cross-phase modulation, by a strong co-propagating wave launched at a different wavelength in the orthogonal polarization [9]).

Considering again "stationary" solutions in the form of Gaussian pulse, $\varphi(x, y) = A\exp(-r^2/l^2)$, one can derive, from Equation (1),

$$u(\xi,\eta) \equiv \frac{U(\xi,\eta)}{A^2} = \frac{4}{A^2 l^2}\left(\xi^2 - \eta^2 - 2\right) - \sigma e^{-2\zeta^2}, \quad (11)$$

where $\xi = x/l$, $\eta = y/l$, $\zeta = r/l$, $r^2 = x^2 + y^2$. It is easy to verify that the norm of function $\varphi(x, y)$ is finite.

In the case of the defocusing nonlinearity, $\sigma = 1$, the potential $u(\xi, \eta)$ has a saddle shape with a well at the center (see Figure 4). The corresponding 2D Gaussian pulse may be stable, provided that it is trapped inside the well. In the case of the self-focusing medium, $\sigma = -1$, the saddle-shaped potential function, $u(\xi, \eta)$, as shown in Figure 4, has an additional local maximum at the center, instead of the well. The maximum appears at $S \equiv Al > \sqrt{2}$, the corresponding Gaussian solution being apparently unstable.

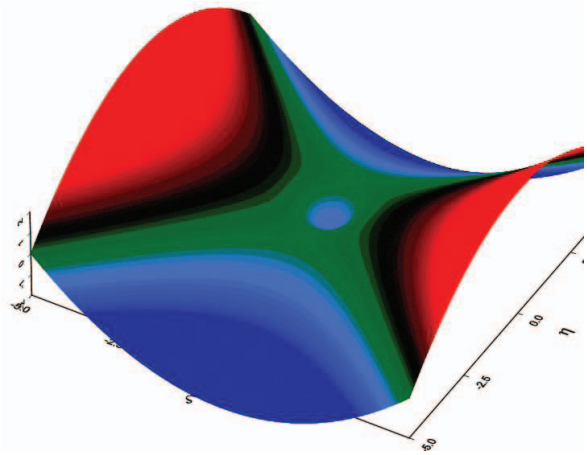

Figure 4: Potential function (11) for $\sigma = 1$ and $S = 5$.

References

[1] Y.S. Kivshar, and Agrawal G.P. Agrawal, "Optical Solitons", Academic Press, San Diego, 2003.

[2] B.A. Malomed, Z.H. Wang, P.L. Chu, and G.D. Peng, J. Opt. Soc. Am. B, **16**, 1197, 1999.

[3] I.G. Kondrat'ev, and M.A. Miller, Sov. J. Radio-physics and Quantum Electronics, **9**, 532, 1966.

[4] J. Apel, L.A. Ostrovsky, Y.A. Stepanyants, and J.F. Lynch, J. Acoust. Soc. Am., **121**, 695, 2007.

[5] B.A. Malomed, and Y.A. Stepanyants, Chaos, **20**, 013130, 2010.

[6] R. Grimshaw, A. Slunyaev, and E. Pelinovsky, Chaos, **20**, 013102, 2010.

[7] Y. Wang, and R. Hao, Opt. Commun., **282**, 3995, 2009.

[8] N.K. Efremidis, G.A. Siviloglou, and D.N. Christodoulides, Phys. Lett. A, **373**, 4073, 2009.

[9] A. Shipulin, G. Onishchukov, and B.A. Malomed, J. Opt. Soc. Am. B, **14**, 3393, 1997.